Pflugers Arch - Eur J Physiol (2006) 453:107–116
DOI 10.1007/s00424-006-0107-0

RENAL FUNCTION, BODY FLUIDS

Adaptive downregulation of a quinidine-sensitive cation conductance in renal principal cells of TWIK-1 knockout mice

I. D. Millar · H. C. Taylor · G. J. Cooper · J. D. Kibble · J. Barhanin · L. Robson

Received: 24 April 2006 / Accepted: 16 May 2006 / Published online: 18 July 2006

Abstract TWIK-1, a member of the two-pore domain K^+ channel family, is expressed in brain, kidney, and lung. The aim of this study was to examine the effect of loss of TWIK-1 on the renal cortical collecting duct. Ducts were isolated from wild-type and TWIK-1 knockout mice by enzyme digestion and whole-cell clamp obtained via the basolateral membrane. Current- and voltage-clamp approaches were used to examine K^+ conductances. No difference was observed between intercalated cells from wild-type or knockout ducts. In contrast, knockout principal cells were hyperpolarized compared to wild-type cells and had a reduced membrane conductance. This was a consequence of a fall in a barium-insensitive, quinidine-sensitive conductance (G_{Quin}). G_{Quin} demonstrated outward rectification and had a relatively low K^+ to Na^+ selectivity ratio. Loss of G_{Quin} would be expected to lead to the hyperpolarization observed in knockout ducts by increasing fractional K^+ conductance and Na^+ uptake by the cell. Consistent with this hypothesis, knockout ducts had an increased diameter in comparison to wild-type ducts. These data suggest that G_{Quin} contributes to the resting membrane potential in the cortical collecting duct and that a fall in G_{Quin} could be an adaptive response in TWIK-1 knockout ducts.

Keywords K^+ channels · Kidney · Patch clamp · TWIK-1 · Collecting duct

I. D. Millar · H. C. Taylor · G. J. Cooper · L. Robson (✉)
Department of Biomedical Science,
University of Sheffield,
Sheffield, S10 2TN, UK
e-mail: l.robson@sheffield.ac.uk

J. D. Kibble
Medical Physiology Department,
St. George's University,
St. George's, Grenada, West Indies

J. Barhanin
Institut de Pharmacologie du CNRS,
660 Route des Lucioles, Sophia-Antipolis,
Valbonne 06560, France

Introduction

At a molecular level, three families of K^+ channels have been identified: the voltage-dependent (K_V), the inwardly rectifying (Kir), and the two-pore domain families. Structurally, these families are very different. K_V channel subunits possess six transmembrane spanning domains and one pore region [7]. Kir channels also have one pore region per subunit but only two transmembrane spanning domains [15]. In contrast, the two-pore family of channels has four transmembrane spanning domains and two pore regions. TWIK-1 was the first two-pore family member to be cloned [17]. It is a weak inward rectifier that is inhibited by barium (Ba^{2+}) and may be important in setting the resting membrane potential of cells. In the mouse, TWIK-1 mRNA is particularly abundant in brain and is also observed in kidney and lung [18]. In rat kidney, TWIK-1 protein is found in the proximal tubule, in the thick ascending limb, and in the intercalated cells of the collecting duct [5]. In contrast, in the rabbit, TWIK-1 is observed in the distal nephron [28]. In the mouse, TWIK-1 is expressed both apically and subapically in the proximal tubule [6, 25]. Loss of TWIK-1 is associated with urinary loss of glucose, consistent with a defect in the proximal tubule, and distal nephron compensation [1]. A recent study has also indicated that TWIK-1 loss also affects proximal tubule phosphate handling, with a decreased expression of the NaPi2a phosphate transporter observed in TWIK-1

knockout mice [25]. It is interesting to note that under control conditions, this was not associated with defects in plasma and urinary electrolytes, consistent with renal compensation [25].

In the kidney, K^+ channels play a vital role in maintaining the resting membrane potential, in cell volume regulation, and also in K^+ secretion [22, 29, 32]. A number of renal K^+ channels have been identified at a molecular level. Two of these, ROMK and CCD-IRK_3, fall into the Kir family, while another, TASK-2, belongs to the two-pore domain family [2, 11, 33]. In the principal cells of the cortical collecting duct, a number of K^+ channels have also been functionally identified, and these play a pivotal role in mediating K^+ secretion by the collecting duct. In these cells, transport is driven by the basolateral Na^+/K^+ ATPase, which maintains a low intracellular Na^+ concentration. This provides the driving force for apical Na^+ uptake, which subsequently drives the secretion of K^+ across the apical membrane via ROMK [35]. On the basolateral membrane, K^+ channels play an important role in K^+ recycling, and at least two channels have been identified in rat. A low conductance, Ba^{2+}-sensitive, inwardly rectifying channel is thought to provide the main basolateral K^+ conductance [20]. A molecular candidate for this channel in mouse is CCD-IRK_3 [33]. In addition, there is also an intermediate conductance K^+ channel [10]. Given the suggestion that distal nephron compensation secondary to a proximal tubule defect is observed in TWIK-1 knockout mice, the aim of this study was to examine the effect of loss of TWIK-1 on conductances in mouse cortical collecting ducts by comparing ducts isolated from both wild-type and TWIK-1 knockout mice.

Materials and methods

Animal model

Collecting ducts were isolated from wild-type and TWIK-1 knockout mice (C57/B6 background) of both sexes and over 6 weeks of age. TWIK-1 knockout mice were obtained from Dr. Jacques Barhanin. Homozygous TWIK-1 knockout mice were confirmed by PCR analysis (Lark Technologies, UK).

Tubule isolation

Tubules were isolated using a protocol modified from Schafer et al. [30]. Adult mice were killed by cervical dislocation according to UK legislation. The kidneys were removed and placed in ice-cold Modified Eagle's Medium (MEM). The capsule was removed and a layer of thin (<0.5 mm), tangential slices taken from the cortex. Slices were torn into pieces and placed in a conical flask containing MEM, type-II collagenase (0.5 mg/ml), protease E (0.1 mg/ml), soya bean trypsin/chymotrypsin inhibitor (50 μg/ml), and glycine (5 mM). The flask was incubated at 37°C without agitation. At 10-min intervals, the digestion medium was decanted, the incubation medium recharged, and digestion continued. Decanted medium was placed on ice, and tubules were allowed to settle to the bottom of the tube. The supernatant was gently removed and replaced with ice-cold MEM plus 1% BSA. Tubules were stored on ice until required. Collecting ducts were identified by their bifurcations [30].

Patch experiments

Collecting ducts were placed in a Perspex bath on the stage of an inverted microscope (Olympus IX70) and held in place using two holding pipettes. Standard patch-clamp techniques were employed to investigate whole-cell currents [9]. Voltage protocols were driven from an IBM-compatible computer equipped with a Digidata interface (Axon Instruments, USA) using the pClamp software, Clampex 8 (Axon Instruments, USA). Recordings were made using a List EPC-7 amplifier. To reduce stray capacitance, patch pipettes were coated with Sylgard (Dow Corning, USA). Ducts were superfused using a small volume, fast exchange perfusion system (Automate, Digitimer, UK).

Whole-cell clamp was obtained via the basolateral aspect. Currents were saved directly onto the computer hard disk after low-pass filtering at 5 kHz. In current-clamp experiments, cell current was clamped to zero and the reversal potential (*V*rev) recorded. In voltage-clamp experiments, cell potential was clamped between +100 and −100 mV, in −20 mV steps. Average currents at each potential were derived using Excel 2000. Steady-state currents were recorded at the end of the potential step. *V*rev in voltage-clamp experiments was determined using polynomial regression. Cell area was calculated from the capacity transients seen in response to a 20-mV potential step, with membrane capacitance assumed to be 1 $\mu F/cm^2$. The mean capacitance of wild-type principal cells was 10.5±0.61 pF (n=37). This was not significantly different to the mean capacitance of knockout principal cells, 11.1±0.75 pF (n=29). The pipette solution contained (in millimols per litre): 145 KCl, 10 mannitol, 0.5 EGTA, and 10 HEPES (titrated to pH 7.4 with KOH). The control bath solution contained (in millimols per litre): 135 NaCl, 5 KCl, 2 $CaCl_2$, 1 $MgCl_2$, and 10 HEPES (titrated to pH 7.4 with NaOH). Changes in junction potential were measured using a flowing 3M KCl reference electrode.

Duct diameter and volume regulation

Duct diameter was measured using a digital camera-based system, Soft Cell (Cairn Instruments, UK). This system

utilized the changes in light intensity, which occur at the cell membrane–bath interface to provide markers for duct diameter. Ducts were placed on a poly-L-lysine-coated Perspex bath on an inverted microscope (Nikon TS-100), superfused with control solution containing (in millimols per litre): 112 NaCl, 3 KCl, 2 $CaCl_2$, 1 $MgCl_2$, 60 mannitol, and 10 HEPES (titrated to pH 7.4 with NaOH). Tubules were then exposed to a hypotonic shock by the removal of 40 mM mannitol. Peak diameter was defined as the maximum diameter recorded upon exposure to hypotonic solution. Steady-state diameter was the diameter attained for at least 1 min.

RT-PCR determination of mRNA expression

The expression of TWIK-1 in mouse collecting ducts was examined using RT-PCR on RNA obtained either from collecting ducts sorted from the tubule preparation or from whole cortex tubule samples. Samples were screened for the following gene markers: ENaC (GeneBank Accession number NM011324), gamma-glutamyltransferase 1 (γGT, NM008116), uromodulin (NM009470), and TWIK-1 (NM008430).

Total RNA was extracted from whole cortex tubules or cortical collecting ducts using the NucleoSpin RNA II kit (Macherey–Nagel, Düren, Germany) and first strand cDNA synthesis performed using Superscript II (Invitrogen, Paisley). This was carried out in combination with an oligo dT primer as directed by the manufacturer's instructions. Approximately 2.5 ng of total RNA from whole kidney samples was used in the reverse transcriptase reaction. In isolated collecting ducts experiments, 0.05 ng of RNA was used. For each experiment, a control reaction was performed, in which the Superscript enzyme was omitted. Amplification of cDNA by PCR was performed in a thermocycler (Techne, Stone, Staffordshire) using the enzyme TAQ DNA polymerase (Eppendorf, Cambridge). Oligonucleotide primers were designed to amplify 400–500 bp fragments of ENaC, γGT, uromodulin, and TWIK-1 (the details of individual primers and the expected product sizes are given in Table 1). Whole cortex tubule samples were subjected to 40 cycles, while isolated collected ducts were subjected to 50 cycles, comprising of denaturation for 30 s at 94°C, annealing (see Table 1 for temperature details) for 30 s, and extension for 45 s at 72°C. A final extension phase of 72°C for 10 min was included for all samples. PCR products were separated by electrophoresis on a 2% agarose gel and visualized by ethidium bromide staining under ultraviolet (302-nm) light. To verify the identity of the PCR products, a restriction endonuclease digestion was performed. Details of the enzymes used and the predicted sizes of the product bands are given in Table 1. RT-PCR was repeated at least three times on RNA from three separate extractions.

Solutions

All chemicals were obtained from Sigma. Osmolality of the experimental solutions was checked using a Roebling osmometer and adjusted to 300±1 mOsM kg^{-1} H_2O using mannitol or water as appropriate.

Statistics

Results are presented as mean±SEM. Effects of experimental interventions were assessed by Student's *t* test, and significance was assumed at the 5% level.

Results

Current-clamp experiments

Current clamp was obtained with 135 Na^+ in the bath and 145 K^+ in the pipette. Ducts were then superfused with high K^+ Ringer (substitution of 95 mM NaCl by KCl) to determine K^+ selectivity, 5 mM Ba^{2+} (removal of 10 mM mannitol) to examine blocker sensitivity, or Na^+ gluconate

Table 1 PCR primers information

Primer	Sequence (5′–3′)	Annealing temperature (°C)	Predicted product size (bp)	Restriction endonuclease used	Predicted cut sizes (bp)
EnaC	Sense 5′-GCTCCTGGGGCTACTGCTACTA-3′, antisense 5′-CGGCTCCGGAACCTGTG-3′	55	421	HINF I	160, 260
γGT	Sense 5′-GCGCCAAGGCCTTCTACAAT-3′, antisense 5′-GCGGCTGGGTGGGTGGTTTCAT-3′	55	430	SAC I	370, 60
Uromodulin	Sense 5′-CTGGATGTCCATAGTGACTC-3′, antisense 5′-TGTGGCATAGCAGTTGGTCA-3′	55	400	NCO I	200, 200
TWIK 1	Sense 5′-AGCGTGTCACCGTGCATGTC-3′, antisense 5′-AATGGATGCAGTCAAGACTC-3′	55	591	XHO I	177, 414

(substitution of 100 mM NaCl by Na^+ gluconate) to determine Cl^- selectivity.

In wild-type principal cells, which had a flat appearance, *V*rev was −62.3±1.47 mV (*n*=27). High K^+ reversibly depolarized *V*rev, Table 2, giving a K^+:Na^+ selectivity ratio of 21.6±2.12. Na^+ gluconate gave a small hyperpolarizing shift, while Ba^{2+} reversibly depolarized *V*rev, Table 2. In wild-type intercalated cells, which had a round appearance, *V*rev was −0.61±2.57 mV (*n*=8). Neither bath K^+ nor Ba^{2+} altered *V*rev. However, Na^+ gluconate gave a significant positive shift in *V*rev, Table 2.

There was no significant difference between wild-type and knockout intercalated cells. However, there were several differences between wild-type and knockout principal cells, Table 2. In knockout cells, the *V*rev in NaCl was hyperpolarized, the K^+-induced depolarization was increased, and the K^+:Na^+ selectivity ratio was greater, 28.7± 2.80 (*n*=16). The response to Ba^{2+} was not significantly different.

Voltage-clamp experiments

The hyperpolarized *V*rev in knockout principal cells could be a consequence of either an increased K^+ conductance or loss of a less K^+-selective conductance. To test these possibilities, voltage-clamp experiments were performed. Whole-cell clamp was obtained with 135 Na^+ in the bath and 145 K^+ in the pipette. To determine K^+ selectivity, the cells were superfused with high K^+ (135 mM NaCl replaced with 135 mM KCl). Ba^{2+} sensitivity was determined from the effect of addition of 5 mM Ba^{2+} to the bath (osmolality maintained by mannitol removal). In some experiments, the effect of 5 and 10 mM Ba^{2+} was examined in high K^+ Ringer. Finally, to investigate Ba^{2+}-insensitive currents, 1-mM quinidine was added to the bath in the continued presence of 5 mM Ba^{2+}. Whole-cell conductances were calculated using the Ohm's law, from the current measurements obtained at each potential.

Table 2 V_{rev} measurements from wild-type (WT) and knockout (KO) principal and intercalated cells (mean±SEM)

	WT	KO
Principal cells, V_{rev} (mV)		
NaCl; WT (*n*=27), KO (*n*=16)	−62.3±1.47	−67.0±1.47[a]
KCl	−9.34±0.61	−9.51±1.39
NaCl (wash)	−58.7±1.68	−60.6±2.55
ΔKCl; WT (*n*=27), KO (*n*=16)	+53.0±1.23	+57.3±1.30[a]
ΔNaGluc; WT (*n*=18), KO (*n*=14)	−2.92±1.28	−5.99±1.06
ΔBa^{2+}; WT (*n*=8), KO (*n*=7)	+37.5±2.80	+40.4±3.67
Intercalated cells V_{rev} (mV)		
NaCl; WT (*n*=8), KO (*n*=10)	−0.61±2.57	−0.50±0.90
KCl	−2.81±2.37	−2.65±0.85
NaCl (wash)	−0.86±2.57	−0.11±0.66
ΔKCl; WT (*n*=8), KO (*n*=10)	−2.20±0.55	−2.15±0.34
ΔNaGluc; WT (*n*=8), KO (*n*=10)	+16.0±0.28	+17.4±0.96
ΔBa^{2+}; WT (*n*=8)	0.65±0.65	NT

V_{rev} values obtained from current-clamp experiments in principal and intercalated cells from wild-type (WT) and knockout (KO) tubules, *Δ* indicates the shift in V_{rev} observed with either KCl, Na^+ gluconate, or Ba^{2+}, *NT* indicates not tested

[a]There is a significant difference between the wild-type and knockout data

Total current profile in wild-type and knockout principal cells

In wild-type principal cells, the currents showed a characteristic profile and had a *V*rev of −68.7±1.87 mV (*n*=22), Fig. 1. At steady state, the currents demonstrated strong inward rectification, Fig. 1. The profile of knockout principal cells was the same as wild-type cells, with a *V*rev of −71.0±1.38 mV (*n*=17) and strong inward rectification, Fig. 1. However, although current profiles were similar, in knockout cells, total conductance was reduced.

In wild-type cells, K^+ caused a depolarizing shift in *V*rev from −70.9±1.19 to 0.00±0.26 mV (*n*=19), corresponding to a K^+:Na^+ selectivity ratio of 45.9±5.99, Fig. 2. In knockout cells, the response to K^+ was similar. K^+ shifted the *V*rev from −71.7±1.49 to 0.20±0.29 mV (*n*=18),

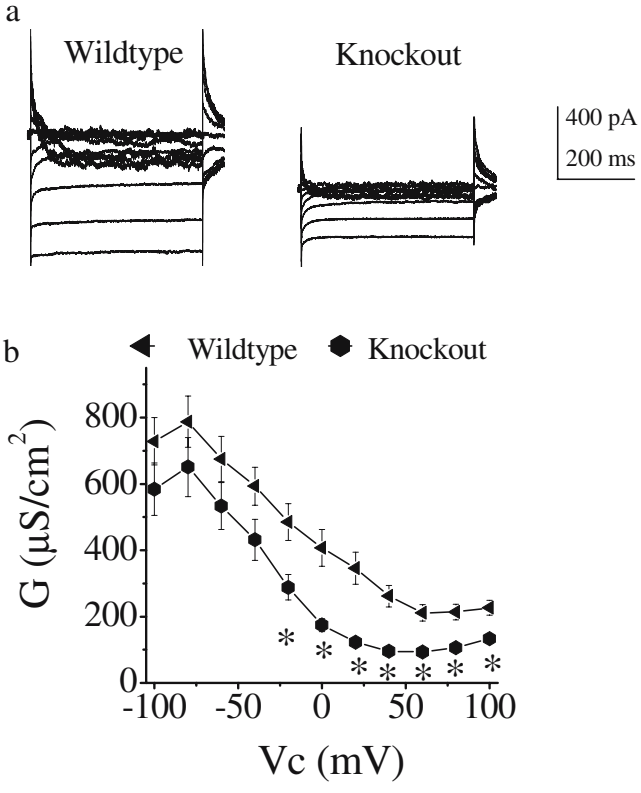

Fig. 1 Current profiles from wild-type and knockout principal cells. **a** Typical traces recorded with Na^+ in the bath from wild-type (*left*) and knockout (*right*) cells. **b** Whole-cell conductance from wild-type (◀, *n*=22) and knockout (⬢, *n*=17) principal cells. *Asterisk symbols* indicate a significant difference to the wild-type data

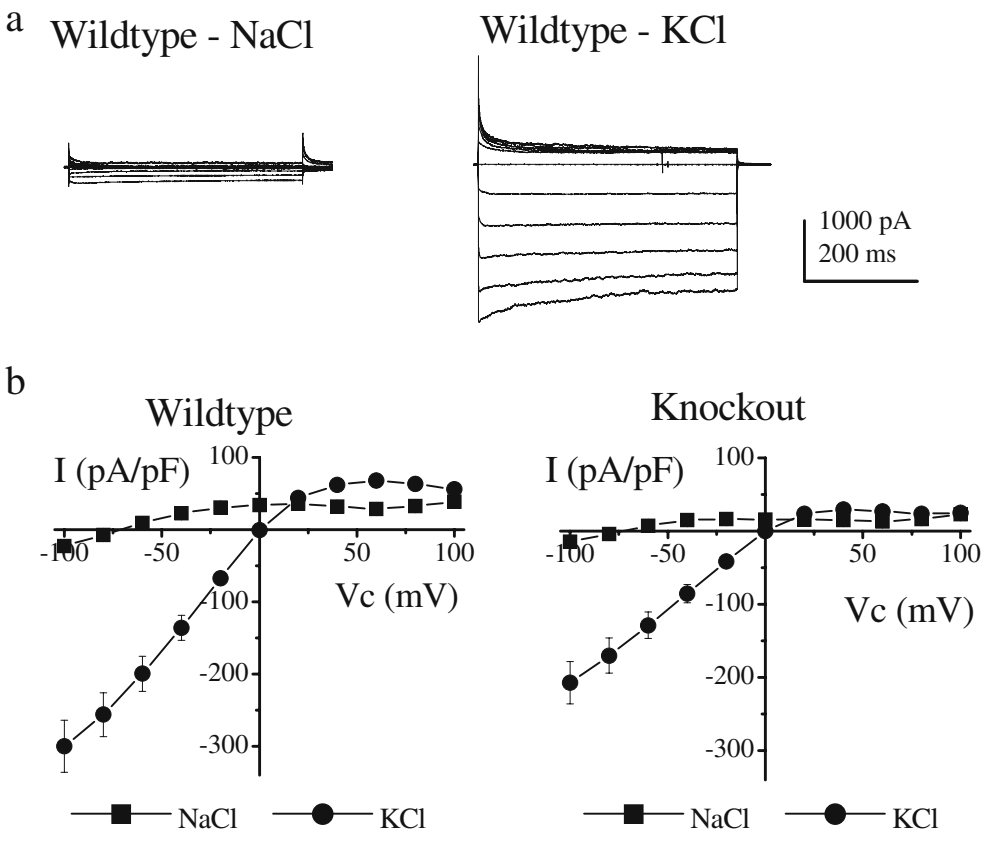

Fig. 2 Effect of substitution of bath Na^+ by K^+. **a** Typical traces recorded from the same wild-type cell with Na^+ (*left*) or K^+ (*right*) in the bath. **b** Mean IV curves in wild-type (*left*, *n*=19) and knockout (*right*, *n*=18) cells. ■ = NaCl and ● = KCl

corresponding to a K^+:Na^+ selectivity ratio of 58.1±9.87, Fig. 2. As with Na^+ in the bath, total cell currents were significantly reduced in knockout cells.

Effect of Ba^{2+}

In wild-type cells with Na^+ in the bath, Ba^{2+} decreased whole-cell currents, shifting the *V*rev from −68.3±3.25 to −22.8±2.57 mV (*n*=13). At +100 mV, the whole-cell current decreased from 37.8±5.87 to 29.9±4.32 pA/pF (*n*=13) in the absence and presence of Ba^{2+}, respectively. At −100 mV, the whole-cell current decreased from −21.4± 2.87 to −7.62±1.37 pA/pF (*n*=13) in the absence and presence of Ba^{2+}, respectively. A similar response was observed in knockout cells, with *V*rev shifting from −71.0± 2.65 to −19.0±4.25 mV (*n*=6). At +100 mV, the whole-cell current decreased from 24.4±3.56 to 19.5±1.58 pA/pF (*n*=6) in the absence and presence of Ba^{2+}, respectively. At −100 mV, the whole-cell current decreased from −19.6± 4.61 to −6.29±1.17 pA/pF (*n*=6) in the absence and presence of Ba^{2+}, respectively.

There was no significant difference in the magnitude of the Ba^{2+}-sensitive conductances between wild-type and knockout cells, 647±109 vs 634±183 μS/cm^2, respectively. The *V*rev of the Ba^{2+}-sensitive currents were also not significantly different, −76.7±2.11 mV (*n*=13) vs −78.5± 0.80 mV (*n*=6) in wild-type and knockout cells, respectively.

With K^+ in the bath, Ba^{2+} also inhibited whole-cell currents in wild-type and knockout cells, Fig. 3a. There was also no significant difference between the Ba^{2+}-sensitive conductances of wild-type and knockout cells, Fig. 3b. However, knockout cells demonstrated a reduced Ba^{2+}-insensitive conductance compared to wild-type cells. This reduction in Ba^{2+}-insensitive conductance was also observed with Na^+ in the bath (data not shown).

To confirm that 5 mM Ba^{2+} gave maximal inhibition, the whole-cell currents were examined in the presence of 5 and 10 mM Ba^{2+} in wild-type cells. 5-mM Ba^{2+} gave a maximal inhibition at all potentials between +20 and −100 mV. At −100 mV, the whole-cell current decreased by 119.6±47.6 and 119.7±47.3 pA/pF (*n*=6) with 5 and 10 mM Ba^{2+}, respectively. Between +40 and +100 mV, 10-mM Ba^{2+} gave a small but significant increase in inhibition. At +100 mV, the whole-cell current decreased by 10.0±3.73 and 12.7±3.71 pA/pF (*n*=6) with 5 and 10 mM Ba^{2+}, respectively.

Effect of 1 mM quinidine in the presence of Ba^{2+}

In wild-type cells, quinidine (added in the continued presence of Ba^{2+}) inhibited whole-cell currents, Fig. 4a.

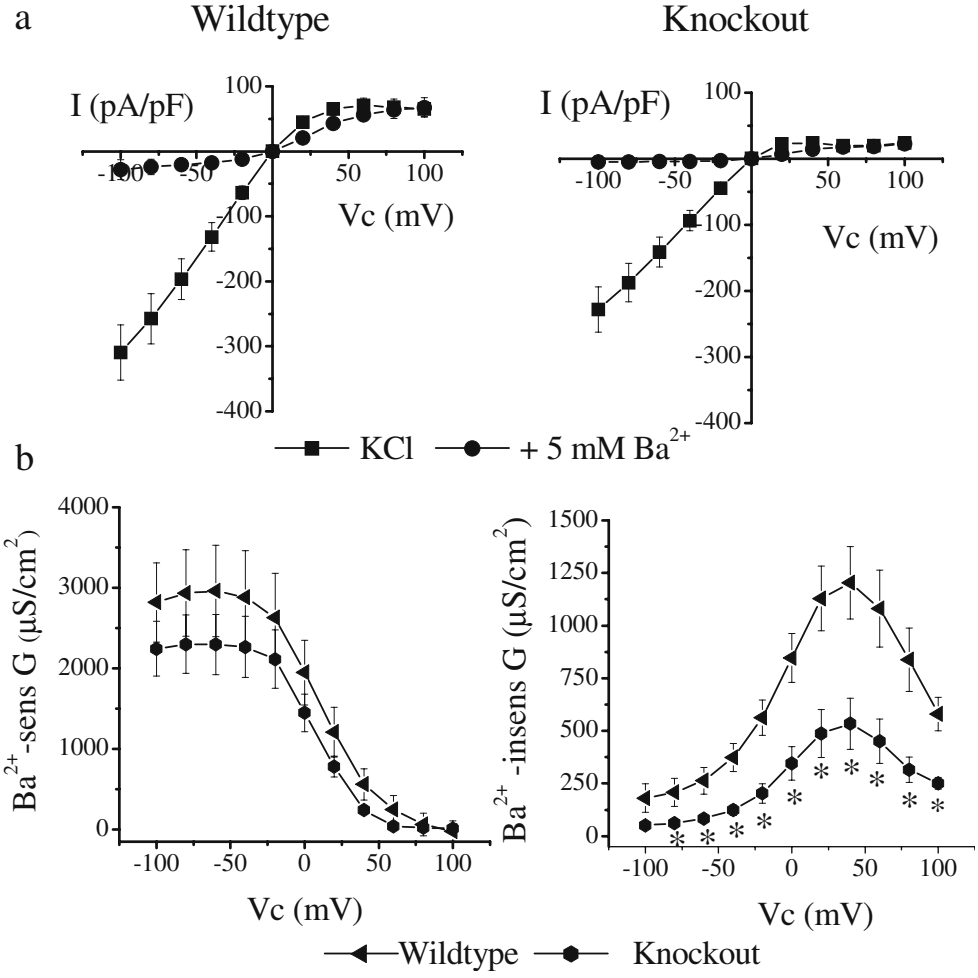

Fig. 3 Effect of 5 mM Ba^{2+} in the presence of extracellular K^+. **a** Currents recorded with K^+ (■) and K^+ plus Ba^{2+} (●) from wild-type (*left*, *n*=13) and knockout (*right*, *n*=6) cells. **b** Ba^{2+}-sensitive conductance (*left*) and Ba^{2+}-insensitive conductances (*right*) from wild-type (◀) and knockout (⬢) principal cells

The quinidine-sensitive conductance (G_{Quin}) demonstrated a biphasic profile. In knockout cells, the response to quinidine was variable, with a significant effect only observed at some potentials, Fig. 4a. The profile of G_{Quin} was similar to the wild-type cells. However, in the knockout cells, G_{Quin} was significantly reduced, Fig. 4b.

Properties of the quinidine-sensitive currents in wild-type principal cells

With Na^+ plus Ba^{2+} or K^+ plus Ba^{2+} in the bath, 1 mM quinidine decreased whole-cell current, Fig. 5a. The *V*rev of the steady-state quinidine-sensitive current in bath Na^+ was −42.4±4.03 mV and in K^+ was 0.97±0.34 mV (*n*=7). This gave a mean shift of 43.4±3.85 mV, corresponding to a K^+:Na^+ selectivity ratio of 7.95±2.40. The quinidine-sensitive currents demonstrated outward rectification, Fig. 5b.

Volume regulation of collecting ducts

Both wild-type and knockout collecting ducts demonstrated volume regulation in response to a hypotonic shock. The control diameter of wild-type tubules was 26.8±0.76 μm (*n*=20). On exposure to hypotonic shock, diameter increased by 1.22±0.12 μm, and this was followed by volume regulation. On achieving steady state after regulation, tubule diameter was 0.44±0.18 μm above the preshock level. In knockout cells, control diameter was 32.2±1.79 μm (*n*=12). This was significantly greater than the control diameter of wild-type tubules. On exposure to a hypotonic shock, the increase to peak was not significantly different to wild-type tubules, 1.54±0.24 μm. In addition, the diameter at steady state after volume regulation was also not significantly different to wild-type tubules, 0.64±0.30 μm.

One possible explanation for the difference between the resting diameters of wild-type and knockout ducts could be due to a different number of measurements taken proximal and distal to the bifurcation, with a distal bifurcation measurement expected to give a higher resting tubule diameter. To address this issue, three diameter measurements were taken from five wild-type collecting ducts (two proximal and one distal to the bifurcation per duct). The mean tubule diameter was 25.7±0.87 μm

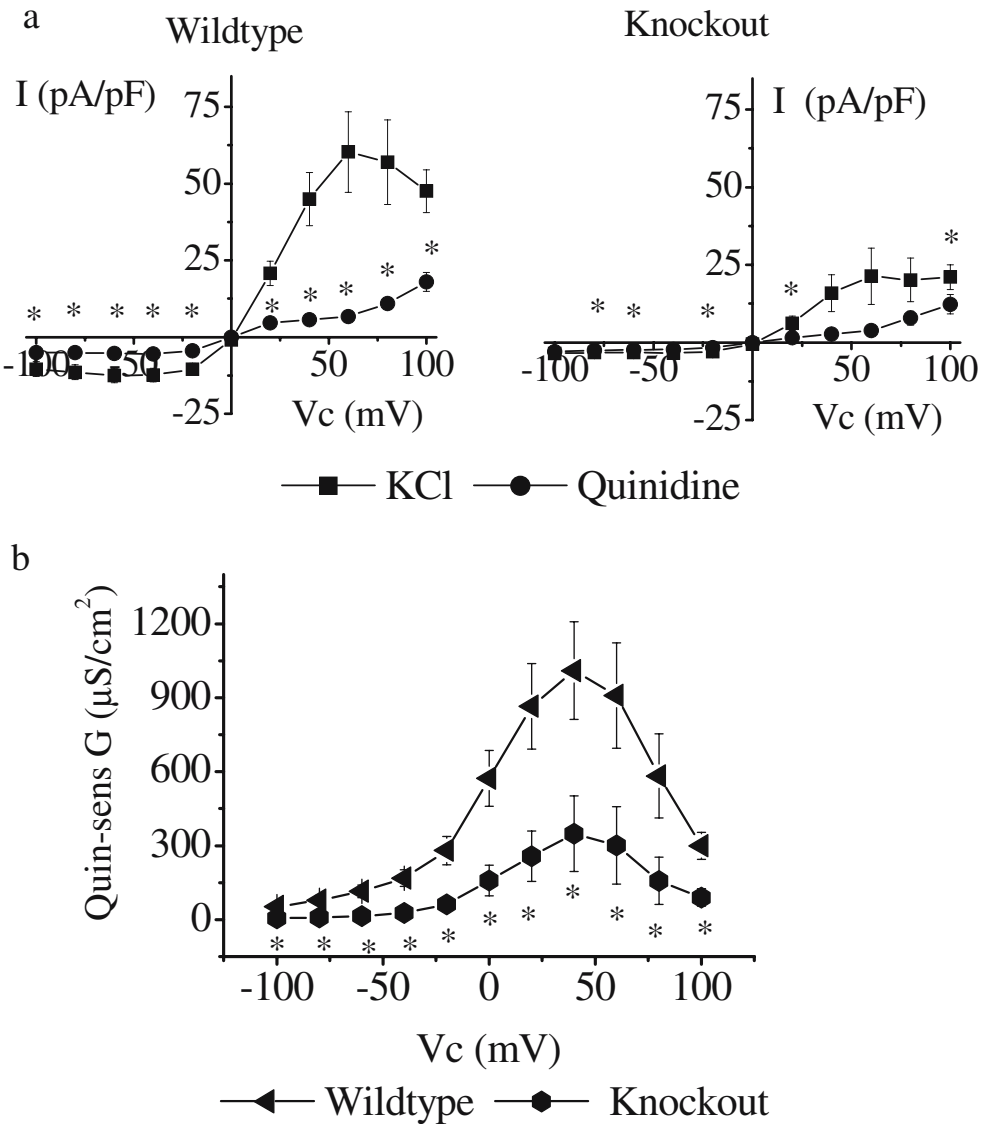

Fig. 4 Effect of quinidine with K^+ and Ba^{2+} in the bath. **a** Currents recorded from wild-type (*left*) or knockout (*right*) cells. ■ = control and ● = plus quinidine. **b** Quinidine-sensitive conductances in wild-type (◀) and knockout (⬢) principal cells. *Asterisk symbols* indicate a significant different to the wild-type data. Wild-type n=11. Knockout n=6

(n=15 measurements from five ducts). This was not significantly different to the resting diameter of wild-type ducts (26.8±0.76 μm, n=20) but was smaller than the diameter observed in knockout ducts (32.2±1.79 μm, n=12).

RT-PCR determination of mRNA expression

In whole cortex tubule samples, the mRNA for ENaC, γGT, uromodulin, and TWIK-1 was identified. Consistent with a collecting duct identity, in tubule samples, only mRNA for ENaC was present. In contrast, mRNA for markers of proximal tubules and thick ascending limbs (γGT and uromodulin, respectively) were absent. In addition, although TWIK-1 mRNA was observed in whole cortex, it was absent from the collecting duct samples, Fig. 6.

Discussion

With whole-cell approaches in intact ducts, the possibility exists that recordings could represent more than one cell. However, the data suggest that recordings represented individual cells. In all patches, capacitance was around 11 pF, lower than the capacitance of single rat principal cells, 29 pF [3], but within the range for the mouse principal M1 cell line, 8 to 14 pF [4, 14]. This lack of electrical coupling is analogous to the nasal epithelium of mice, which demonstrates similar capacitance measurements in cell clusters of different sizes [31].

Recordings from collecting ducts showed two different electrophysiological profiles. In one group of cells, which demonstrated a round morphology, the dominant conductance was a Cl^- conductance. In these cells, the Vrev was close to the Nernst potential for Cl^-, and neither K^+ nor Ba^{2+}

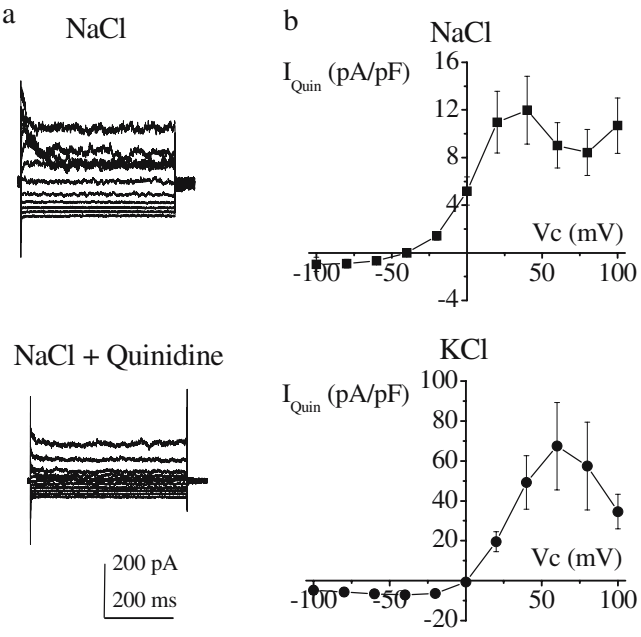

Fig. 5 Quinidine-sensitive currents in wild-type cells. 5 mM Ba^{2+} present at all times. **a** Typical whole-cell traces recorded with NaCl plus Ba^{2+} in the absence (*upper*) and presence (*lower*) of quinidine. **b** Mean quinidine-sensitive currents with bath Na^+ plus Ba^{2+} (*upper*, n=7) or K^+ plus Ba^{2+} (*lower*, n=7)

had any effect. Substitution of bath Cl^- by gluconate shifted the *V*rev in a positive direction, indicating Cl^- selectivity. These data are consistent with intercalated cells in the collecting duct [24]. In contrast, a K^+ conductance was dominant in the second group of cells, which had a flat appearance. The *V*rev in these cells followed the Nernst potential for K^+, and Ba^{2+} gave a depolarizing shift in *V*rev, consistent with inhibition of a K^+ conductance. The shift in *V*rev with bath gluconate did not follow the Nernst potential for Cl^-, indicating that in this second population of cells, any Cl^- conductance was small or absent. This profile suggests that the second population of cells is attributable to principal cells [13]. The identification of principal and intercalated cells based on K^+ or Cl^- selectivity is supported by a recent single channel study, which demonstrated that K^+ and Cl^- channels are found in different cell populations in the collecting duct [26]. In addition, rat collecting duct principal cells studied using the whole-cell patch-clamp technique also have a high K^+ conductance, while intercalated cells have a high Cl^- conductance [8].

In the intercalated cells, loss of TWIK-1 was without effect, with no difference between wild-type and knockout cells. A previous study in rat has shown that there is expression of TWIK-1 in intercalated cells [5]. However, a recent study suggests that in the mouse, TWIK-1 is expressed in the proximal tubule [6]. The electrophysiological data obtained in this study are consistent with a lack of expression of TWIK-1 in intercalated cells in the mouse. In contrast, differences were observed in the principal cells. Knockout principal cells had a hyperpolarized *V*rev, demonstrated a greater shift in *V*rev in response to bath K^+, and had a greater K^+:Na^+ selectivity ratio. Voltage-clamp data demonstrated that this hyperpolarization was due to a reduction in a poorly K^+-selective cation conductance in the knockout cells.

The total currents recorded in wild-type and knockout cortical collecting duct principal cells demonstrated a similar profile. However, the magnitude of the total conductance in TWIK-1 knockout cells was reduced in comparison to the wild-type cells. One possible candidate for the reduced conductance is the loss of TWIK-1. However, there are several pieces of evidence that do not support this hypothesis. In the first instance, TWIK-1 is a Ba^{2+}-sensitive conductance [17]. In the current study, Ba^{2+} inhibited currents in both wild-type and knockout cells. However, there was no difference between the magnitudes

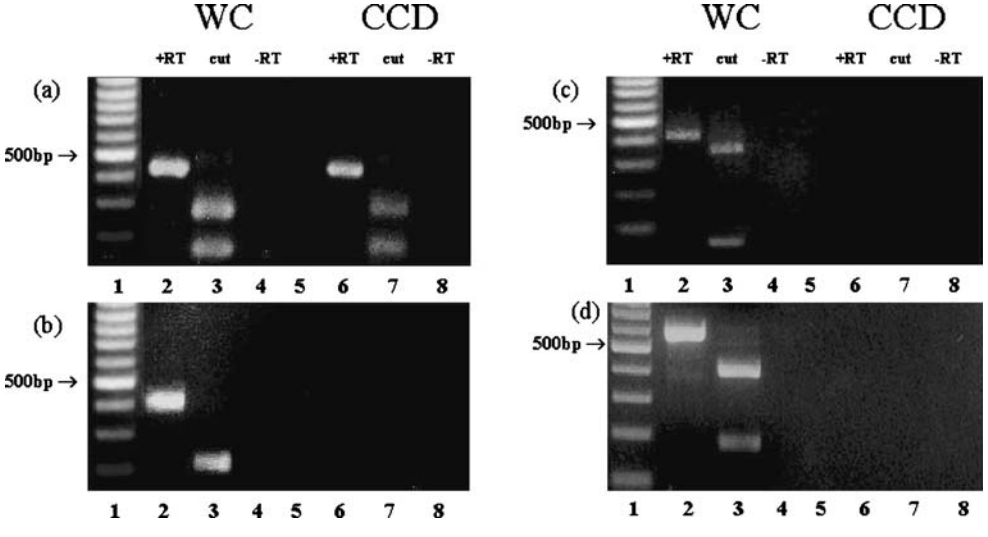

Fig. 6 Whole cortex (*WC*) and cortical collecting duct (*CCD*) expression of mRNA. Products amplified by PCR in the presence (*RT*+) or absence (*RT*–) of reverse transcriptase enzyme are shown in *panels* **a**–**d**. cDNA identity was confirmed by digestion of PCR products using restriction endonuclease (*cut*). Primers were used to amplify ENaC (**a**), uromodulin (**b**), γGT (**c**), and TWIK-1 (**d**) (see Table 1). The *left-hand lane* of *each panel* shows a 100-bp ladder (Fermentas, Sunderland), and the 500-bp marker is indicated

of the Ba^{2+}-sensitive conductances. Rather, it was the Ba^{2+}-insensitive conductances that showed a difference. TWIK-1 is also highly K^+-selective [17]. However, the selectivity of the reduced conductance was only eight times more selective for K^+ over Na^+. Again, this property is not consistent with TWIK-1. In contrast to TWIK-1, the reduced conductance demonstrated outward rectification. Finally, mRNA for TWIK-1 was absent from cortical collecting duct samples but was present in whole kidney.

Although Ba^{2+}-insensitive, the conductance was inhibited by quinidine, with the quinidine-sensitive conductance (G_{Quin}) in knockout cells significantly reduced compared to wild-type cells. G_{Quin} showed strong outward rectification. This profile was present in both wild-type and knockout cells, suggesting that there was a reduction in the magnitude of the conductance rather than a complete loss. Consistent with the hyperpolarization seen in knockout cells, G_{Quin} was only eight times more selective for K^+ over Na^+.

A number of K^+ channels have been identified in the collecting duct. The most studied K^+ channel to date is ROMK, which is found on the apical membrane of the principal cells of the cortical collecting duct. ROMK is an inwardly rectifying, Ba^{2+}-sensitive channel that is highly K^+-selective [11]. For this reason, it cannot be attributable to G_{Quin}, although it could form part of the Ba^{2+}-sensitive currents described earlier. CCD-IRK_3 is also found in the cortical collecting duct, this time on the basolateral membrane. Like ROMK, it is an inward rectifier, highly K^+-selective, and inhibited by Ba^{2+} [33]. Again, it cannot be represented by G_{Quin} but could form part of the Ba^{2+}-sensitive currents. Other K^+ channels described in the basolateral membrane of the rat cortical collecting duct include small conductance and intermediate conductance K^+ channels [10, 20]. However, these are either quinidine-insensitive (small conductance) or blocked by Ba^{2+} (intermediate conductance) and therefore do not fit with G_{Quin}.

Although G_{Quin} has a higher selectivity to K^+ vs Na^+, it acts as a cation channel, and previous studies in a number of collecting duct models have described a variety of cation channels. In rat cortical collecting duct cell lines, two cation channels have been described in the apical membrane [12, 16], with similar channels observed in mouse, rat, and rabbit medullary collecting ducts [19, 21, 27, 34]. Unlike G_{Quin}, which is around eight times more selective for K^+ over Na^+, the majority of these channels do not discriminate well between Na^+ and K^+. Although, one cation channel described in mouse inner medullary collecting duct cells is five times more selective for K^+ over Na^+ [21]. Such a K^+-selective cation conductance has also been described in the apical membrane of rabbit proximal tubules [23].

At the resting membrane potential, the net current flow through G_{Quin} will be inward and composed of a small outward K^+ current and a larger inward Na^+ current. However, as G_{Quin} is an outward rectifier, the net inward flow of current will be small. G_{Quin} is therefore unlikely to play a role in K^+ loss or in the movement of Na^+ into the cell. Instead, it is more likely to be involved in fine-tuning of the resting membrane potential. In wild-type cells, G_{Quin} contributed around 6% of the total whole-cell conductance (37±9 $\mu S/cm^2$) at −60 mV, while the Ba^{2+}-sensitive conductance contributed around 92% of the total (602± 88 $\mu S/cm^2$). Therefore, G_{Quin} contributes only a small fraction of the total conductance. However, despite this small contribution, the reduction of G_{Quin} in knockout cells was associated with a hyperpolarization of the potential in whole-cell patches, with a shift in *V*rev of around 8%. This hyperpolarization would be expected to reduce the driving force for the efflux of K^+ and increase the driving force for Na^+ entry into the cells. Such changes in cation movement may explain the increase in diameter observed in knockout tubules at rest. The loss of TWIK-1 is associated with defects in proximal tubule handling of phosphate [25]. Therefore, it would be expected that a greater amount of Na^+ would be delivered to the collecting duct under this circumstance. The downregulation of G_{Quin} and the subsequent hyperpolarization of the principal cells could reflect an adaptive response in the knockout mice, which acts to minimize the urinary loss of Na^+ in the absence of TWIK-1.

In conclusion, these data indicate that loss of TWIK-1 leads to a reduction in a quinidine-sensitive cation conductance in principal cells of the cortical collecting duct of mouse. The conductance, G_{Quin}, is eight times more selective for K^+ over Na^+. G_{Quin} is not sensitive to Ba^{2+} and demonstrates outward rectification. Loss of TWIK-1 was also associated with an increase in cortical collecting duct diameter. Taken together, these data suggest that G_{Quin} may play an important role in fine-tuning the resting membrane potential in cortical collecting duct principal cells.

Acknowledgements We gratefully acknowledge the support of the BBSRC and the Physiological Society. I.D. Millar is currently at the Faculty of Life Sciences, University of Manchester.

References

1. Barhanin J, Arrighi I, Barriere H, Poujeol P, Tauc M, Vallon V, Warth R (2003) Epithelial K^+ channels in transgenic mice. Fed Eur Physiol Soc S23–3 (Abstr)
2. Barriere H, Belfodil R, Rubera I, Tauc M, Lesage F, Poujeol C, Guy N, Barhanin J, Poujeol P (2003) Role of TASK2 potassium channels regarding volume regulation in primary cultures of mouse proximal tubules. J Gen Physiol 122:177–190
3. Bubien JK (1995) Whole cell sodium conductance of principal cells freshly isolated from rat cortical collecting duct. Am J Physiol 269:C791–C796

4. Chalfant ML, O'Brien TG, Civan MM (1996) Whole cell and unitary amiloride- sensitive sodium currents in M-l mouse cortical collecting duct cells. Am J Physiol 270:C998–C1010
5. Cluzeaud F, Reyes R, Escoubet B, Fay M, Lazdunski M, Bonvalet JP, Lesage F, Farman N (1998) Expression of TWIK-1, a novel weakly inward rectifying potassium channel in rat kidney. Am J Physiol 275:C1602–C1609
6. Decressac S, Franco M, Bendahhou S, Warth R, Knauer S, Barhanin J, Lazdunski M, Lesage F (2004) ARF6-dependent interaction of the TWIK1 K^+ channel with EFA6, a GDP/GTP Exchange Factor for ARF6. EMBO Rep 5:1171–1175
7. Doyle DA, Cabral JM, Pfuetzner RA, Kuo A, Gulbis JM, Cohen SL, Chait BT, MacKinnon R (1998) The structure of the potassium channel: molecular basis of K^+ conduction and selectivity. Science 280:69–77
8. Gray DA, Frindt G, Zhang Y-Y, Palmer LG (2005) Basolateral K^+ conductance in principal cells of rat CCD. Am J Physiol 288:493–504
9. Hamill OP, Marty A, Neher E, Sakmann B, Sigworth FJ (1981) Improved patch clamp techniques for high resolution current recording from cells and cell free membrane patches. Pflugers Arch 391:85–100
10. Hirsch J, Schlatter E (1993) K^+ channels in the basolateral membrane of rat cortical collecting duct. Pflugers Arch 424:470–477
11. Ho K, Nichols CG, Lederer WJ, Lytton J, Vassilev PM, Kanazirska MV, Hebert SC (1993) Cloning and expression of an inwardly rectifying ATP-regulated potassium channel. Nature 362:31–38
12. Huber SM, Horster MF (1996) Ontogeny of apical membrane ion conductances and channel expression in cortical collecting duct cells. Am J Physiol 271:F698–F708
13. Koeppen BM, Biagi BA, Giebisch G (1983) Intracellular microelectrode characterization of the rabbit cortical collecting duct. Am J Physiol 244:F35–F47
14. Korbmacher C, Segal AS, Fejes-Toth G, Giebisch G, Boulpaep EL (1993) Whole-cell currents in single and confluent M-1 mouse cortical collecting duct cells. J Gen Physiol 102:761–793
15. Kubo Y, Baldwin TJ, Jan YN, Jan LY (1993) Primary structure and functional expression of a mouse inward rectifier potassium channel. Nature 362:127–133
16. Laskowski FH, Christine CW, Gitter AH, Beyenbach KW, Gross P, Fromter E (1990) Cation channels in the apical membrane of collecting duct principal cell epithelium in culture. Ren Physiol Biochem 13:70–81
17. Lesage F, Guillemare E, Fink M, Duprat F, Lazdunski M, Romey G, Barhanin J (1996) TWIK-1, a ubiquitous human weakly inward rectifying K^+ channel with a novel structure. EMBO J 15:1004–1011
18. Lesage F, Lauritzen I, Duprat F, Reyes R, Fink M, Heurteaux C, Lazdunski M (1997) The structure, function and distribution of the mouse TWIK-1 K^+ channel. FEBS Lett 402:28–32
19. Light DB, McCann FV, Keller TM, Stanton BA (1988) Amiloride-sensitive cation channel in apical membrane of inner medullary collecting duct. Am J Physiol 255:F278–F286
20. Lu M, Wang W-H (1996) Nitric oxide regulates the low conductance K^+ channel in basolateral membrane of cortical collecting duct. Am J Physiol 270:C1336–C1342
21. Luo Y, Vassilev PM, Li X, Kawanabe Y, Zhou J (2003) Native polycystin-2 functions as a plasma membrane Ca^{2+}-permeable cation channel in renal epithelium. Mol Cell Biol 23:2600–2607
22. Macri P, Breton S, Beck JS, Cardinal J, Laprade R (1993) Basolateral K^+, Cl^- and HCO_3^- conductances and cell volume regulation in the rabbit proximal convoluted tubule. Am J Physiol 264:F365–F376
23. Marom S, Dagan D, Winaver J, Palti Y (1989) Brush-border membrane cation conducting channels from rat kidney proximal tubules. Am J Physiol 257:F328–F335
24. Muto S, Yasoshima K, Yoshitomi K, Imai M, Asano Y (1990) Electrophysiological identification of α- and β-intercalated cells and their distribution along the rabbit distal nephron segments. J Clin Invest 86:1829–1839
25. Nie X, Arrighi I, Kaissling B, Pfaff I, Mann J, Barhanin J, Vallon V (2005) Expression and insights on function of potassium channel TWIK-1 in mouse kidney. Pflugers Arch 451:479–488
26. Nissant A, Paulais M, Lachheb S, Lourdel S, Teulon J (2006) Similar chloride channels in the connecting tubule and cortical collecting duct of the mouse kidney. Am J Physiol Renal Physiol 290:F1421–F1429
27. Ono S, Mougouris T, DuBose TD, Sansom SC (1994) ATP and calcium modulation of nonselective cation channels in IMCD cells. Am J Physiol 267:F558–F565
28. Orias M, Velasquez H, Tung F, Lee G, Desir G (1997) Cloning and localization of a double-pore K^+ channel, KCNK1: exclusive expression in distal nephron segments. Am J Physiol 273:F663–F666
29. Sansom SC, Mougouris T, Ono S, DuBose TD (1994) ATP-sensitive K^+-selective channels of inner medullary collecting duct cells. Am J Physiol 267:F489–F496
30. Schafer JA, Watkins L, Li L, Herter P, Haxelmans S, Schlatter E (1998) A simplified method for isolated of large numbers of defined nephron segments. Am J Physiol 273:F650–F657
31. Tarran R, Gray MA, Evans MJ, Colledge WH, Ratcliff R, Argent BE (1998) Basal chloride currents in murine airway epithelial cells: modulation by CFTR. Am J Physiol 274:C904–C913
32. Vallon V, Grahammer F, Richter K, Bleich M, Lang F, Barhanin J, Volkl H, Warth R (2001) Role of KCNE1-dependent K^+ fluxes in mouse proximal tubule. J Am Soc Nephrol 12:2003–2011
33. Welling PA (1997) Primary structure and functional expression of a cortical collecting duct Kir channel. Am J Physiol 273:F825–F836
34. Xia S-L, Noh S-H, Verlander JW, Gelband CH, Wingo CS (2001) Apical membrane of native $OMCD_i$ cells has nonselective cation channels. Am J Physiol 281:F48–F55
35. Xu JZ, Hall AE, Peterson LN, Bienkowski MJ, Eessalu TE, Hebert SC (1997) Localization of the ROMK protein on apical membranes of rat kidney nephron segments. Am J Physiol 273:739–748